The Status of VIRGO

F.Acernese[6], P.Amico[10], M. Al-Shourbagy[11], S.Aoudia[7], S. Avino[6], D.Babusci[4], G.Ballardin[2], F.Barone[6], L.Barsotti[11], M.Barsuglia[8], F.Beauville[1], M.A.Bizouard[8], C.Boccara[9], F.Bondu[7], L.Bosi[10], C.Bradaschia[11], S.Braccini[11], S. Birindelli[11], A.Brillet[7], V.Brisson[8], L.Brocco[12], D.Buskulic[1], E.Calloni[6], E.Campagna[3], F.Cavalier[8], R.Cavalieri[2], G.Cella[11], E.Chassande-Mottin[7], C. Corda[11], A.-C.Clapson[8], F.Cleva[7], J.-P.Coulon[7], E.Cuoco[2], V.Dattilo[2], M.Davier[8], R.De Rosa[6], L.Di Fiore[6], A.Di Virgilio[11], B.Dujardin[7], A.Eleuteri[6], D.Enard[2], I.Ferrante[11], F.Fidecaro[11], I.Fiori[11], R.Flaminio[1,2] , J.-D.Fournier[7], O.François, S.Frasca[12], F.Frasconi[2;11], A. Freise[2], L.Gammaitoni[10], A.Gennai[11], A.Giazotto[11], G.Giordano[4], L. Giordano[6], R. Gouaty[1], D. Grosjean[1], G.Guidi[3], S.Hebri[2], H.Heitmann[7], P.Hello[8], L.Holloway[2], S. Karkar[1], S.Kreckelbergh[8], P.La Penna[2], N.Letendre[1], V.Loriette[9], M.Loupias[2], G.Losurdo[3], J.-M.Mackowski[5], E.Majorana[12] , C.N.Man[7], M. Mantovani[11], F. Marchesoni[10], F.Marion[1], J. Marque[2], F.Martelli[3], A.Masserot[1], M.Mazzoni[3], L.Milano[6], C. Moins[2], J.Moreau[9], N.Morgado[5], B.Mours[1], A. Pai[12], C.Palomba[12], F.Paoletti[2;11], S. Pardi[6], A. Pasqualetti[2], R.Passaquieti[11], D.Passuello[11], B.Perniola[3], F. Piergiovanni[3], L.Pinard[5], R.Poggiani[11], M.Punturo[10], P.Puppo[12], K.Qipiani[6], P.Rapagnani[12], V.Reita[9], A.Remillieux[5], F.Ricci[12], I.Ricciardi[6], P. Ruggi[2], G.Russo[6], S.Solimeno[6], A. Spallicci[7], R.Stanga[3], R. Taddei[2], M. Tonelli[11], A. Toncelli[11], E.Tournefier[1], F.Travasso[10], G. Vajente[11], D.Verkindt[1], F.Vetrano[3], A.Viceré[3], J.-Y.Vinet[7], H.Vocca[10], M.Yvert[1], Z. Zhang[2]

[1]*Laboratoire d'Annecy-le-Vieux de physique des particules, Annecy-le-Vieux, France*
[2]*European Gravitational Observatory (EGO), Cascina (Pi) Italia*
[3]*INFN, Sezione di Firenze/Urbino, Sesto Fiorentino, and/or Università di Firenze, and/or Università di Urbino, Italia*
[4] *INFN, Laboratori Nazionali di Frascati, Frascati (Rm), Italia*
[5]*LMA, Villeurbanne, Lyon, France*
[6]*INFN, sezione di Napoli and/or Università di Napoli "Federico II" Complesso Universitario di Monte S.Angelo, Italia and/or Università di Salerno, Fisciano (Sa), Italia*
[7] *Departement Artemis - Observatoire Cote d'Azur, Nice , Cedex 4, France*
[8]*LAL, IN2P3/CNRS-Univ. De Paris-Sud, Orsay , France*
[9]*ESPCI, Paris, France*
[10]*INFN Sezione di Perugia and/or Università di Perugia, Perugia, Italia*
[11]*INFN, Sezione di Pisa and/or Università di Pisa, Pisa, Italia*
[12]*INFN, Sezione di Roma and/or Università "La Sapienza", Roma, Italia*

Corresponding author e-mail address: paolo.lapenna@ego-gw.it

Abstract.

The VIRGO interferometer commissioning started in September 2003. Through several steps of increasing complexity, in August 2005 all the components and systems of the interferometer were functioning. The activity is presently aimed to upgrade some parts of the detector to reach the design sensitivity. The status of advancement of VIRGO and the short-term plans are discussed here.

1. Introduction

The gravitational wave detector VIRGO, supported by *CNRS* (France) and *INFN* (Italy), consists mainly of a recycled Michelson interferometer where each arm is replaced by a 3 km long Fabry-Perot cavity [1]. A passing gravitational wave can be detected by the interferometric measurement of the induced change of the two arm length difference. VIRGO is located at the European

Gravitational Observatory (EGO), close to Cascina (Pisa, Italy), and is designed to detect gravitational waves emitted by astrophysical sources in the frequency range between a few Hz and a few kHz. Other detectors presently in action, such as LIGO [2], TAMA [3] and GEO [4], are based upon to the same principle.

2. VIRGO design

2.1 The injection system

The VIRGO optical layout is sketched in Fig.1. A 20 W laser beam @ 1064 nm is produced by a *Nd:YVO*$_4$ high power injection laser and locked to a solid state 700mW *Nd:YAG* master laser. After passing on the optical table (DT) to be correctly aligned to the interferometer the beam enters the vacuum system reaching the suspended input optical bench (IB). The beam is then spatially filtered by a 144 m long suspended triangular cavity (*input mode cleaner* - IMC) before being injected into the main interferometer. The IMC is used as a reference in the pre-stabilization loop, where the laser frequency is stabilized within a few Hz by using the standard Pound-Drever-Hall technique [5]. The frequency stability below 15 Hz is achieved by an additional control system that stabilizes the length of the IMC with respect to a rigid 30 cm-long *reference cavity* (RFC), located on the IB and made by a material with very low thermal expansion coefficient (ULE).

2.2 Optical Layout

The laser, whose nominal power is 20 W, is presently running at 17 W, but only 0.7 W are injected into the interferometer (*itf*) in order to strongly reduce spurious effects induced by back-scattered light into the IMC (see below). The beam passes through the PR (*power recycling*) mirror, is separated by the BS (*beam splitter*) and enters the two long Fabry-Perot cavities (*North* and *West* cavity) with a finesse of 49 (North Arm) and 50 (West Arm). They enhance the light path, amplifying the beam phase change induced by the arm length variation.
The itf is set on the dark fringe. This means that, apart from losses and the small amount of light transmitted by the terminal mirrors, all the light fed-in by the injection system returns to it. PR is a 92.2% reflecting mirror sending back the light returning to the laser port in order to create a Fabry-Perot cavity between it and the Michelson itf. In this way the power impinging onto the BS is amplified up to a factor 50 (the present *recycling factor* is around 35).
The main output signal is reconstructed by a set of high-quantum efficiency InGaAs photodiodes (B1), assembled on a bench outside of the vacuum system (EB). The output beam, before reaching B1, passes through a monolithic 2.5 cm long cavity (*output mode cleaner* - OMC) located on a bench suspended in a vacuum (DB) and designed to filter higher order optical modes originating from misalignments and optical defects.

2.3 Mirror suspensions

Each mirror is suspended to a multi-stage seismic isolator (*superattenuator, SA*) [6] designed to filter ground seismic vibrations by ten-twelve orders of magnitude in all the degrees of freedom, starting from a few Hz. Above 4 Hz the residual seismic noise at the mirror level turns out to be smaller the thermal noise floor, expected to limit the VIRGO sensitivity below a few hundreds of Hz [7]. The SA consists of a pre-isolator stage (a 6 m-long *inverted pendulum*) at which is attached a chain of six *seismic filters*. The mirror and its *reference mass* are both suspended to a *marionette*, attached to the last filter of the chain by a steel wire [8]. Longitudinal and angular forces can be applied to the mirror by four coils located on the reference mass acting on facing permanent magnets attached to the mirror. Longitudinal and angular forces can be applied at the level of the marionette in a similar way.
The pitch and yaw motions of each suspended mirror are reduced from several microrads down to fractions of microrad by a digital feedback system using a ground-based camera as a monitor and marionette coils as actuators [9] (*local controls,* LC). This angular stability allows the pre-alignment of the beams in the interferometer and the achievement of a stable interference pattern.

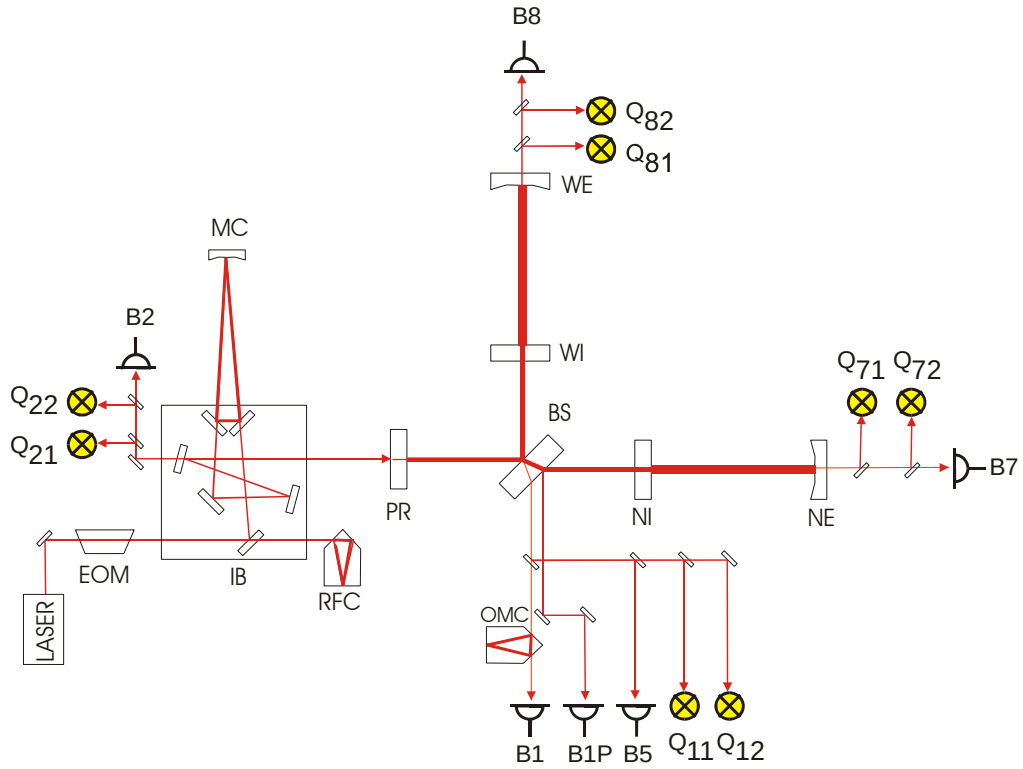

Fig.1: VIRGO optical layout.

3. The Commissioning of the interferometer

3.1 Local Controls

Pitch and yaw motions of each suspended mirror are damped by a digital feedback (*local controls*). The marionette angular displacements (monitored by an optical lever impinging onto a ground-based PSD sensor) are chilled by feedback torques from the marionette coils [8]. The accomplished angular stability (a fraction of μrad) allows in the Summer 2003 the pre-alignment of the itf and the achievement of a good interference pattern.

3.2 Interferometer longitudinal control

After the pre-alignment, the itf has to be "locked" in the longitudinal working position starting from swinging mirrors. This means to have the laser light resonating in the Fabry-Perot and recycling cavities, with the main output port on the dark fringe. The mirrors are locked in the correct longitudinal position by using the Pound-Drever-Hall technique [5] and reconstructing all the relevant lengths by using the error signals coming from photodiodes placed at different output ports. The photodiode signals are digitized and sent via optical links to the *global control system* [9] that computes at a 10 kHz sampling rate the correction signals sent to the mirror suspension actuators. Once the locking is achieved, the laser frequency is stabilized on the "*common mode*", that is the sum of the two long arm lengths (*second stage frequency stabilization*). This is a very stable reference in the entire VIRGO band. The photodiode B5 (Fig.1) yields the error signal for the control of the two arm common length. The laser frequency is stabilized to the common mode by adding B5 signal to the IMC error signal used for the frequency pre-stabilization (see [10] for a detailed scheme).

VIRGO commissioning started in September 2003 with the locking of the single Fabry-Perot cavities at resonance. In February 2004 the itf was locked for the first time in the *recombined* mode, that means to have the two long cavities locked at the resonance (by acting upon the end mirrors), the itf locked on the dark fringe (by controlling the BS position), while PR mirror is kept

misaligned. The main difficulties were encountered in the full itf locking. Indeed, once the PR mirror is aligned, a large amount of light is backscattered into the injection system, increasing the beam frequency noise and making the locking impossible. As mentioned above, in order to reduce the amount of this spurious light we decided to operate with a reduced input power (0.7 W instead of the available 7 W). A new injection bench is presently under construction; a Faraday isolator located on the bench will suppress the light back-scattered into the IMC, allowing to run the itf with the maximum power. In addition, during the shutdown, the compounded power recycling mirror (exhibiting spurious resonances, affecting the lock acquisition and inducing noise peaks in the itf) will be replaced by a monolithic one.
VIRGO uses a completely original locking technique (the variable finesse technique), widely described elsewhere [11]. In short, a preliminary locking acquisition is achieved with the PR misaligned by 10 μrads, avoiding in this way the backscattering problem during the most critical part, that is to chill the swinging mirrors in the correct position. In October 2004 the locking of the recycled itf was acquired for the first time.

3.3 The Automatic Alignment

Once the itf is locked it is necessary to maintain the mirrors aligned with one another and with respect to the beam with a high level of accuracy (rms close to 10^{-9} rad), not achievable by the ground-based local controls. In the recombined itf this was accomplished by using the Anderson technique [12]. Error signals from quadrant photodiodes at different output ports (Fig.1) are managed by the global control system in order to provide suitable correction signals to be sent to coil-magnets actuators of the marionette [13]. Even if the control band is below a few Hz, aggressive roll-off filters are necessary to destroy the noise injected in the region of some tens of Hz. The main problem to close the automatic alignment loops on the entire itf are the fluctuations of the sensing matrix (giving the pitch and yaw displacements of each mirror from the quadrant signals) induced by slow mirror misalignments. Moreover jumps in the recycling cavity power were observed. These sudden jumps, occurring with different periods (few seconds or few minutes) are possibly linked to different parameters like spurious beams in the itf, alignment of mirrors and photodiodes, etc., which create some virtual working point as read through the photodiode error signal, leading thus to a kind of variable bi-stability. This made the locking less robust, slowing down the activities in this year. In July a full realignment of the injection system and the implementation of a mirror *drift angular control* (with a few tenths of mHz band) is expected to improve the stability of the itf.

3.4 *Mirror Hierarchical Control*

An active control of the inverted pendulum top stage (*inertial damping*) is employed on each suspension to damp its normal modes (from a few tens of mHz to 2 Hz) [14]. This reduces the mirror swing down to a few tenths of μm/s, which is enough for allowing locking acquisition. Also the compensation force to be applied to the mirror from the reference mass coils to maintain the itf locked are decreased. This allows us to reduce the reference mass coil DAC noise in the detection band, a floor proportional to the maximum voltage made available at the mirror level. For the same reason the large (hundreds of microns) drifts of the mirror (below a few tens of mHz) are compensated by acting upon the suspension top stage (*tidal control*). Once the tidal control is implemented, the mirror residual displacement is around 1 μm peak to peak. This displacement, occurring mainly below a few Hz, is compensated acting upon the marionette so that the DAC noise is filtered by the mirror pendulum below. Only nanometer displacements are compensated directly at the mirror level from the reference mass (above a few Hz). This *hierarchical control* [15], already implemented on the recombined itf, will allow us to reduce the control noise floor below the planned antenna sensitivity.

3.5 *Status report*

Seven commissioning runs have been performed so far. The corresponding configurations are reported here below, while the sensitivity curves are displayed in Fig.2.

C1 (14-17 Nov. 03) –: North cavity locked at resonance.
C2 (20-23 Feb. 04) –: North cavity locked at resonance plus automatic alignment.
C3 (26-27 Apr.04) –: C2 with second stage frequency stabilization (23-26 Apr.04) and recombined interferometer. The sensitivity curve in Fig.2 is referred to the recombined configuration.
C4 (24-29 June 04) –: Recombined interferometer with automatic alignment, second stage frequency stabilization and tidal control.
C5 – As in C4 with suspension hierarchical control (2-6 Dec.04) and first data taking with recycled interferometer (6-7 Dec.04). The sensitivity curve in Fig.2 is referred to the recycled configuration.
C6 (29 July–12 August 05) –: As in C5, with alignment drift control active on PR, NI, WI, WE on tx and ty d.o.f. automatic alignment active on NE, alfa technique on, permament calibration lines on.
C7 (14-19 Sept. 05) –: As in C6, with DAC noise reduction, tidal control on BS, BS coil drivers in low noise configuration, new control of PR mirror, increased modulation depth, and ITF AA fully working on 10 d.o.f.: all the parts and systems of the interferometer are working.

The cyan curve in Fig.2 concerns the best sensitivity curve ever achieved. The improvement in C7 with respect to C6 is ascribed to the automatic alignment (up to about 30 Hz), to the reduction of the beam splitter control noise and of the DAC noise (up to about 200 Hz), to the improvement in the PR mirror control (up to about 500 Hz) and to some photodiode read-out configuration change (in the high frequency range). In addition to the sensitivity curve measurements, C6 (15 days long) has shown that the interferometer can be operated in science mode for a long term (maximum lock of 40 hours) with a good duty cycle (about 90%), and C7 run has demonstrated the full functioning of all the components, systems and control loops of the interferometer.

4. Data Analysis Activities

The data acquisition chain was successfully tested during the commissioning runs. The current data rate is 7 Mbytes/s of compressed data. A data analysis group is focused on the calibration of the apparatus with the goal of reconstructing the gravitational wave signal starting from different itf outputs. The main potential sources of gravitational waves are searched inside different working groups: coalescing binaries, burst, periodic and stochastic background. The coalescing binaries and burst data analysis pipelines are now used on the real data [16] [17]. An effort to characterize the VIRGO noise is carried out, in particular by the *noise group* that aims to identify sources of non stationarity and non-gaussianity, masking the detection.
A LIGO-VIRGO working group was settled up to perform a joint analysis for bursts and coalescing binaries detection by the data exchange [18]. A collaboration with Italian bar detector researchers (*Auriga*, *Explorer* and *Nautilus*) was also settled up for burst and stochastic background searches.

5. Short-term Plans

In September 2005 the interferometer will be shut down in order to install a new injection bench. Thanks to the presence of a Faraday isolator the troubles induced by the light backscattered from the interferometer into the input mode cleaner will disappear. Presently this backscattering problem forced us to operate with a reduced input power (0.7 W instead of the nominal 10 W) in order to reduce the backscattered light. The increase of the power should allow to decrease the shot-noise floor, limiting the antenna sensitivity above a few hundreds of Hz and to reach, in this frequency range, the target sensitivity. After the restart, the put in action of the suspension hierarchical control (already tested) will allow decreasing the DAC noise affecting the sensitivity in the region of some hundreds of Hz. The reaching of the design sensitivity between 10 Hz and 100 Hz will require the reduction of the noise introduced in the apparatus by the locking and alignment loops.

The commissioning activities are expected to restart in December 2005.

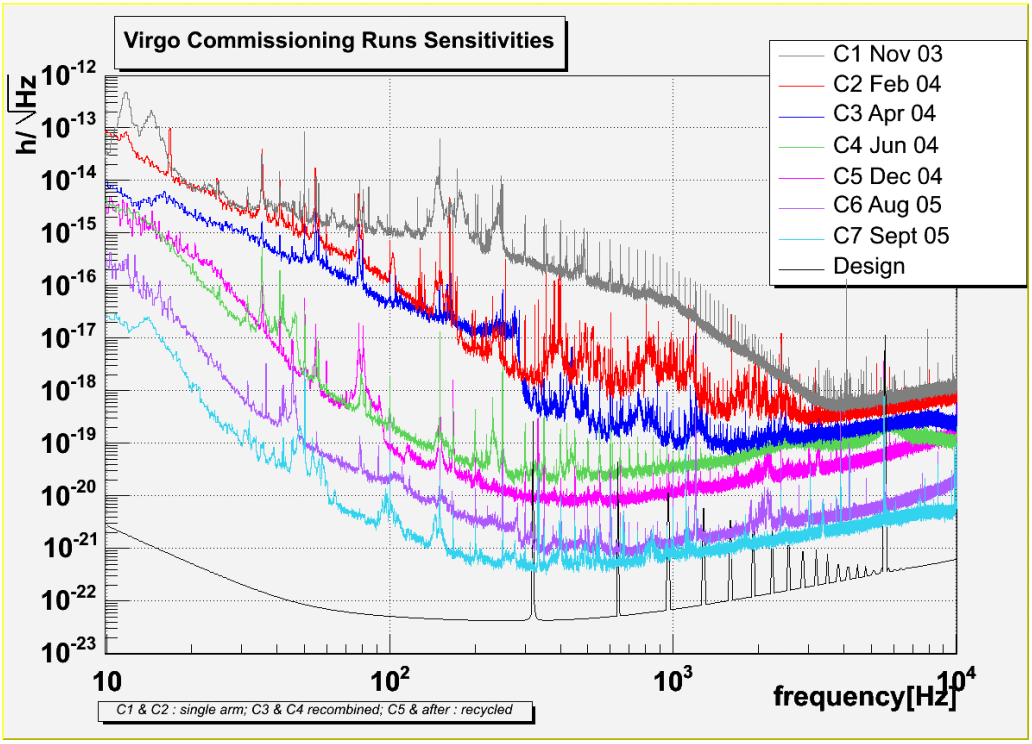

Fig.2: VIRGO sensitivity curves in the different runs compared with the designed one.

References

[1] http://www.virgo.infn.it.
[2] D.Sigg, *Proceedings of the 6th Amaldi Conference.*
[3] M.-K.Fujimoto, *Proceedings of the 6th Amaldi Conference.*
[4] H.Lueck, *Proceedings of the 6th Amaldi Conference.*
[5] R.W.P.Drever *et al., Appl. Phys. B : Photophys. Laser Chem.,* 31, 97-105 (1983).
[6] G.Ballardin *et al*., *Rev. Sci. Instrum.,* 79 (9), 3643-3652 (2001).
[7] S.Braccini *et al*., *Astrop. Phys.,* 23 (6), 557-565 (2005).
[8] A.Bernardini *et al.*, *Rev. Sci. Instrum.,*72, 3463 (1999).
[9] F.Acernese *et al.*, *Astrop. Phys.,* 20, 617-628 (2004).
[10] L.Barsotti *for the VIRGO collaboration*, *Proceedings of the 6th Amaldi Conference.*
[11] F.Cavalier, *Le controle global de Virgo,* These d'Habilitation a diriger des Recherches, Universitè de Paris Sud, LAL 01-69 (2001).
[12] G.Losurdo *et al.*, *Rev. Sci. Instrum.,* 79 (9), 3653-3661 (2001).
[13] D.Z.Anderson, *Appl. Opt.,* 23, 2944-2949 (1984).
[14] M.Mantovani *for the VIRGO collaboration*, *Proceedings of the 6th Amaldi Conference.*
[15] F.Acernese *et al.*, *Astrop. Phys.,* 20 (6), 629-640 (2004).
[16] A.Viceré *for the VIRGO collaboration*, *Proceedings of the 6th Amaldi Conference.*
[17] C.Clapson *for the VIRGO collaboration*, *Proceedings of the 6th Amaldi Conference.*
[18] S. Fairhurst *for the LIGO-Virgo joint working group*, *Proceedings of the 6th Amaldi Conference.*